



THREE-DIMENSIONAL SEISMIC ISOLATOR BY FLUID LEVITATION AND ITS PERFORMANCE EXPERIMENTS WITH E-DEFENSE

M. Yamada ⁽¹⁾, K. Kajiwara ⁽²⁾, E. Sato ⁽³⁾, T. Horiuchi ⁽⁴⁾, H. Kase ⁽⁵⁾,
M. Hayatsu ⁽⁶⁾, T. Tomizawa ⁽⁷⁾, M. Yasuda ⁽⁸⁾

⁽¹⁾ Research Fellow, E-Defense, National Research Institute for Earth Science and Disaster Resilience, m-yamada@bosai.go.jp

⁽²⁾ Director, E-Defense, National Research Institute for Earth Science and Disaster Resilience, kaji@bosai.go.jp

⁽³⁾ Chief Researcher, E-Defense, National Research Institute for Earth Science and Disaster Resilience, ejji@bosai.go.jp

⁽⁴⁾ Research Fellow, E-Defense, National Research Institute for Earth Science and Disaster Resilience, thori@bosai.go.jp

⁽⁵⁾ Mechanical Designer, Engineering Department, Nemoto Project Industry Co., Ltd. h-kase@nemoto-kikaku.com

⁽⁶⁾ Senior Chief Engineer, Development Center, Hitachi Plant Mechanics Co., Ltd. masaki.hayatsu.wz@hitachi.com

⁽⁷⁾ Senior Assistant Professor, Department of Architecture, School of Science and Technology, Meiji University, tomizawa@meiji.ac.jp

⁽⁸⁾ Professor, Department of Mechanical Engineering, Setsunan University, ma-yasud@mec.setsunan.ac.jp

Abstract

This paper describes a newly developed 3D seismic isolation device using coil springs and negative stiffness linkages in parallel on fluid levitation pads and its seismic excitation experiments using the Three-Dimensional (3D) Full-Scale Earthquake Testing Facility (E-Defense). The fluid levitation pads were designed under the fluid bearing formula and the design was verified through experiments with two types of fluids, that is, air and water. The target value of vibration reduction was set to 4 or less in the seismic intensity by the Japan Meteorological Agency (JMA), where few damages occur in the infrastructure. As a result of the experiments by using JR Takatori (The 1995 Great Hanshin-Awaji Earthquake) as the input wave, the JMA seismic intensity of the base-isolated structure was 4, and the acceleration responses of the isolated structure was successfully reduced to 1/10 in the horizontal direction and 1/3 in the vertical direction with both air and water. Also, we confirmed that levitation pads did not make any contacts with the floor surface even in the high level of vertical accelerations and operated stably by monitoring the levitation height during excitations.

Keywords: Earthquake; Three-dimensional seismic isolation; Fluid levitation; Negative stiffness; Vibration

1. Introduction

In 2018, many disasters occurred consecutively in various parts of Japan. In particular, the earthquakes that hit the northern part of Osaka Prefecture on June 18 and the eastern Iburi region, Hokkaido Prefecture on September 6 caused damages to wide areas. In Hokkaido, electricity has stopped in almost all areas. Damages to infrastructure such as roads, railways, telecommunications, and water supplies were reported [1]. For reducing such damages, we are making efforts to realize a “Zero earthquake damage areas including infrastructure” that is an effective way for protecting safety and security of people. An example of this concept, seismic isolation block, is shown in **Fig.1**. The advantage of seismic isolation block is that the block can continue economic activities and perform more functions than evacuation zones and reconstruction bases in the event of an earthquake. We have been developing a series of high-performance 3D seismic isolation systems (from Prototype No. 1 to Prototype No. 4, at this moment) since 2016 [2~5]. The latest Prototype No.4 was achieved a support load of 10 tons. The horizontal seismic isolation is made with a levitation system consisting of fluid-ejection pads that can cut off the structure-floor contact. It is noted that the levitation height was set to around 40 μ m to reduce the volume of injected fluid and thus save energy. The vertical seismic isolation is made with a system consisting of a



Fig. 1 – Seismic isolation block concept



low stiffness support using coil springs and negative stiffness linkages in parallel. This paper describes the full-scale seismic excitation experiments on the new 3D seismic isolation.

2. Target Performance of 3D seismic isolator

At the starting stage of the development, we have to define the target performance. As described above, the purpose of this development is to realize the area that continues economic activities even after large earthquakes. In most of infrastructures (gas supplies, elevators, etc.), operation suspensions and/or inspections are required after earthquakes with JMA seismic intensity of Lower 5 or larger. Therefore, the seismic intensity 4 or less on the seismic isolation device was set as the current target value. It is noted that the Japan Meteorological Agency (JMA) seismic intensity class is an index unique to Japan and expresses the magnitude of earthquake in 10 levels based on 3D acceleration time history data. The detection value of the accelerometer is adjusted to the human sense by emphasizing the periodic component that has a large effect on buildings and humans. **Fig.2** shows the relationship between the period and acceleration of the earthquake and the seismic intensity.

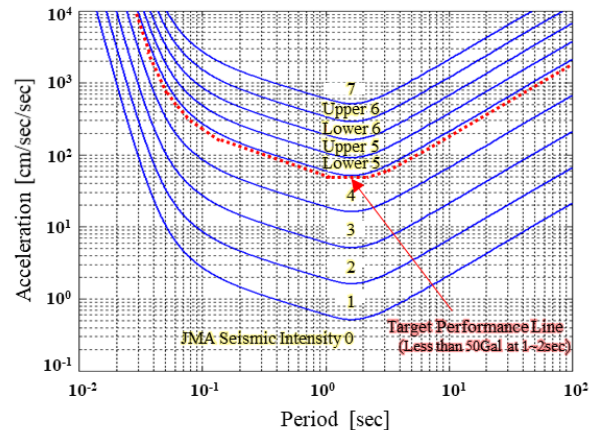


Fig. 2 – Relationship between earthquake period, acceleration, the JMA seismic intensity (theoretical value, When the vibration of a uniform cycle continues for several second) and target performance line of 3D seismic isolation device


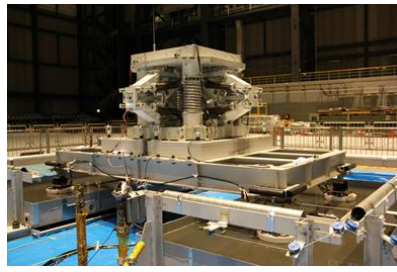

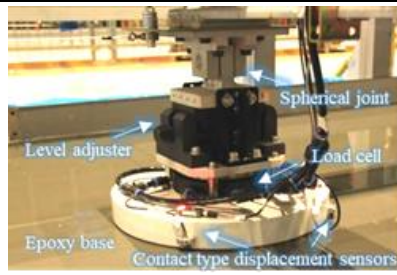
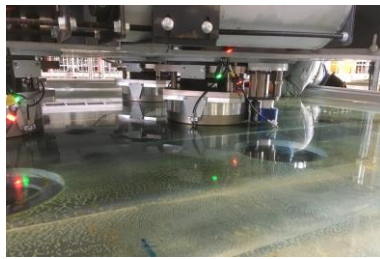
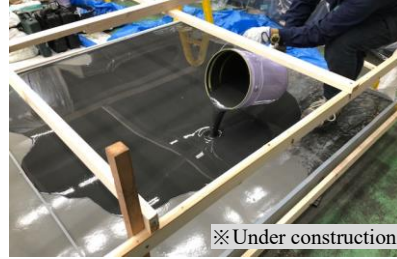
Created with reference to the JMA website
<https://www.data.jma.go.jp/svd/eqev/data/kyoshin/kaisetsu/comp.htm>

3. Design of seismic isolation system

Table 1 shows the specifications of prototypes No. 4. Those of the previous prototype No.3 are also shown for emphasizing the characteristics of prototype No.4. No.4 had distributed legs to support the entire structure and the width and depth of the seismic isolation device were set to 2: 1 rectangle considering actual applications. The supporting load increased from 3,200 kg in No. 3 to 10,000 kg in No. 4. This time, we focused on the development of horizontal seismic isolation, so we decided to use the same system for vertical seismic isolation as No. 3. The vertical seismic isolation setup has a half footprint area of No.4, so we can experiment with changing the center of gravity depending on the mounting location of the vertical isolation setup. This is important information when applying to actual equipment. The vertical isolation setup by itself was too light, so it was mounted on the center or end of the No. 4 frame with a weight of about 7,000 kg. The horizontal seismic isolation system is a fluid levitation type characterized by extremely low friction in a non-periodic sliding bearing. In order to reduce the fluid flow, the levitation height was set to 40 μm . Although the fluid used in the Prototype No. 1-3 was compressed air. We found that high-pressure air has a high risk of accidents and is subject to various regulations under the High Pressure Gas Safety Act in Japan in the future development of large-scale systems. Therefore, water was selected as a new fluid that can be highly pressurized and has no risk of fire. This time, two types of levitation pads with the same diameter were prepared and their performances were compared. As described in detail elsewhere [4], these two pads achieved a low coefficient of friction of 1 / 5,000 or less. The levitating surface was made with a high-flow epoxy under a self-leveling construction method in which a high-flow epoxy resin was poured onto a concrete slab and solidified like the water surface. The vertical seismic isolation consists of the negative stiffness link mechanism and the coil spring which are arranged in parallel so that it can reduce the spring constant while support a large load [5]. Thereby, the natural period in the vertical direction is designed to 3 sec or more that is long enough to cut off earthquake excitations. We understand rocking motion is a major issue in 3D seismic isolation. We believe the rocking motion can be suppressed because the horizontal vibration is greatly reduced.



Table 1 – Outline of 3D seismic isolation system

	Prototype No.3	Prototype No.4
Overview		
Levitation pad		
Surface / Base		
Over the vertical isolation weight	2,000 kg	2,000 kg
Over the Horizontal isolation weight	3,200 kg	10,000 kg
Stroke	± 65cm (H), ± 20cm (V)	± 75cm (H), ± 20cm (V)
Levitation pad	280mm in diameter × 4units (Air)	450mm in diameter × 4units (Air or Water)
Body and pad joint	Silicon rubber	Spherical joint & Level adjuster
Surface / Base	Tempered glass / Steel frame	Epoxy resin / Concrete slab

※ (H) : Horizontal direction, (V) : Vertical direction

4. Single-unit experiment of levitation pad

4.1 Design of air levitation pad

The shape of the air levitation pad in **Fig.3**. Eight nozzles with orifices are provided at half the radial direction of the pad. The air levitation pad of No.4 is designed by the same design method [5] as No.3. The design is performed by firstly determining the approximate pad diameter from the load to be isolated and the air pressure that can be supplied, and then determining the orifice diameter that provides the required levitation height with a small air flow. Note that the larger the diameter of the levitation pad, the lower capability of the utilities such as pumps, but there is a trade-off with the cost of manufacturing a flat surface that does not contact the floor. Also, the smaller the diameter of the orifice, the higher the stiffness of the pad in the vertical direction. However, the pressure and flow required for levitation decrease, and the pad does not levitate. For this reason, we considered the orifice diameter that satisfies the levitation height, supply pressure, and supply flow rate while taking into account the capacity of the utility for air pressure supply.



The method of designing the orifice diameter after determining the diameter of the air levitation pad is as follows. First, find the pressure distribution required to levitate the air levitation pad. The target load is 10,000kg (10t), and therefore the supporting load of each pad is 2,500kg. The pressure distribution $P_a(r)$ in the radial direction r of the pad is described in Eq. (1) where P_{ai} is the outlet pressure of the orifice, P_{atm} (atmospheric pressure) is the outlet pressure of the air levitation pad, r_{a1} is the distance from the center of the pad to the orifice, r_{a2} is the radius of the air levitation pad.

$$P_a(r) = P_{atm} \sqrt{1 - \left(1 - \frac{P_{ai}^2}{P_{atm}^2}\right) \cdot \frac{\ln\left(\frac{r}{r_{a2}}\right)}{\ln\left(\frac{r_{a1}}{r_{a2}}\right)}} \quad (1)$$

The pressure distribution in the radial direction r of the pad is shown in Fig.4. The orifice outlet pressure P_{ai} at which the supporting load (integral value in the circumferential direction) is 2,500 kg is 0.351 MPa (absolute pressure). Next, find the mass flow rate of air flowing through each orifice. The mass flow rate G_0 can be written as Eq. (2) where the outflow velocity coefficient is Φ (P_{ai} / P_{as}), the supply pressure is P_{as} , the outlet pressure of the orifice is P_{ai} , the orifice coefficient is α_a (empirically 0.1), the diameter of the orifice is d_a , the gas constant of air is R , and temperature is T_{emp} .

$$G_0 = \Phi(P_{ai} / P_{as}) \cdot \alpha_a \cdot \left(\frac{\pi d_a^2}{4}\right) \cdot \frac{P_{as}}{\sqrt{RT_{emp}}} \quad (2)$$

When P_{ai} / P_{as} is 0.53 or less, the nozzle speed becomes sonic and the mass flow rate is constant (choked flow). The outflow velocity coefficient at this time is 0.69. The outflow velocity coefficient with P_{ai} / P_{as} of 0.53 or more can be expressed in Eq. (3) by assuming the specific heat ratio κ .

$$\Phi(P_{ai} / P_{as}) = \sqrt{\frac{2\kappa \cdot \left(\left(\frac{P_{ai}}{P_{as}}\right)^{2/\kappa} - \left(\frac{P_{ai}}{P_{as}}\right)^{\kappa+1/\kappa}\right)}{\kappa - 1}} \quad (3)$$

The relationship between the pressure ratio P_{ai} / P_{as} and the outflow velocity coefficient Φ (P_{ai} / P_{as}) is shown in Fig.5. Considering the stability of the levitation and the efficiency of the utility, it was designed with $P_{ai} / P_{as} = 0.53$, where the mass flow rate is constant. On the other hand, the mass flow rate G_m of the air flowing out of the gap between the porous air levitation pads can be written in Eq. (4) where the density is ρ_a , the levitation height is h_a , the outlet pressure of the orifice is P_{ai} , and the outlet pressure of the air levitation pad is P_{atm} (atmospheric pressure).

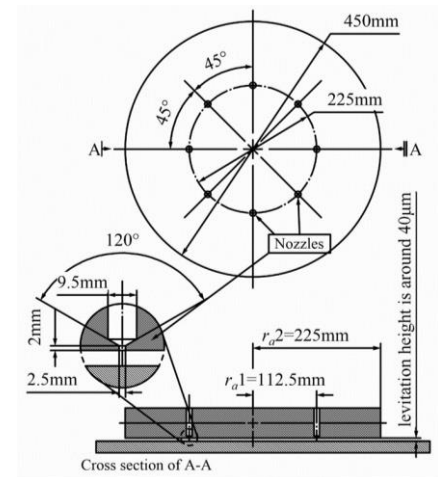


Fig. 3 – Design of the air levitation pad

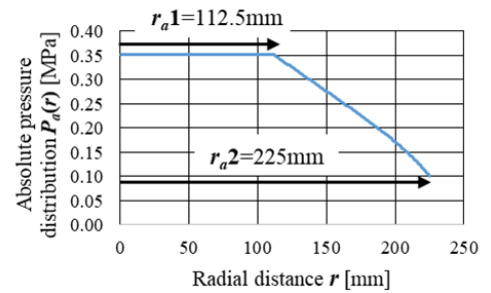


Fig. 4 – Absolute pressure distribution of air levitation pad

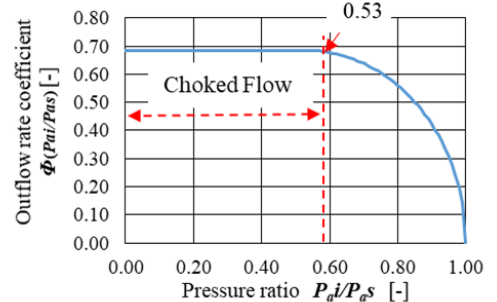


Fig. 5 – Relationship between pressure ratio and outflow rate coefficient



$$G_m = \frac{\pi \rho_a h_a^3 P_{atm} \cdot \left(1 - \frac{P_{ai}^2}{P_{atm}^2}\right)}{12\mu_a \cdot \ln\left(\frac{r_{a1}}{r_{a2}}\right)} \quad (4)$$

The orifice diameter was determined under the condition that the mass flow rate of air through the eight orifices, $8 \cdot G_0$, and the mass flow rate of air flowing between the levitation pad and the floor surface, G_m , were the same. In addition, the levitation height was set to 50 μm or more. The supply pressure was set to 0.7 MPa or less due to utility restrictions. As a result, the orifice diameter was set to 2.5 mm. The mass flow rate G_m is converted to the volume flow rate Q_a , and compared with the value of the flow rate sensor in the experiment in Section 4.2. These design parameters are summarized in **Table 2**.

Table 2 Parameter for design of air levitation pad

Item	Symbol	Value	Item	Symbol	Value
Support load	W	2,500 kg	Air density	ρ_a	1.209 kg/m ³
Number of nozzles	N	8	Air viscosity	μ_a	1.86 $\times 10^{-5}$ Pa sec
Supply pressure (Gauge)	P_{as}	0.65 MPa	Levitation pad diameter	$2 \cdot r_{a2}$	450 mm
Orifice coefficient	α_a	0.1	Nozzle position diameter	$2 \cdot r_{a1}$	225 mm
Temperature	T_{emp}	293 K	Orifice diameter	d_a	2.5 mm
Gas constant	R	287.1 J/(kgK)	Volume of flow rate	Q_a	329 L/min
Specific heat ratio	K	1.4	Levitation height	h_a	63 μm

4.2 Design of water levitation pad

The shape of the water levitation pad is shown in **Fig.6**. The water levitation pad had the same diameter and number of nozzles as the air levitation pad. The difference from the air levitation pad is that a pocket is provided to ensure initial levitation. The pockets are provided with partitions to generate restoring force when the water levitation pad is inclined. The pressure distribution $P_w(r)$ in the radial direction r of the water levitation pad can be written in **Eq. (5)** based on a viscous flow equation from the Navier-Stokes equation in the cylindrical coordinate system by assuming that the flow velocity in the vertical direction when flowing through the gap was zero, the pressure was constant in the vertical direction, and the differential term in the radial direction was sufficiently small.

$$P_w(r) = P_{wi} \sqrt{1 - \frac{\ln\left(\frac{r}{r_{w1}}\right)}{\ln\left(\frac{r_{w2}}{r_{w1}}\right)}} \quad (5)$$

Where P_{wi} is the outlet pressure of the orifice and r_{w1} is the radius of air levitation pad.

The pressure distribution in the radial direction r of the pad is shown in **Fig.7**. The orifice outlet pressure P_{wi} at which the supporting load (integral value in the circumferential direction) is becomes 2,500 kg is 0.226 MPa (gauge pressure).

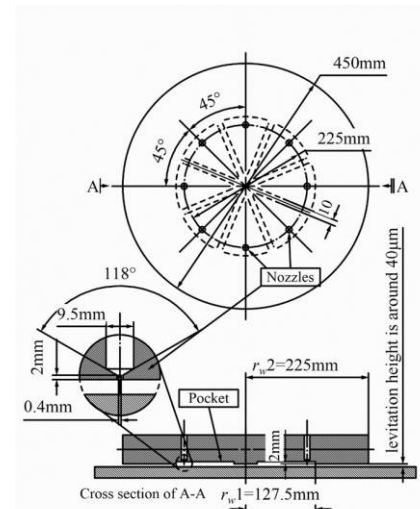


Fig. 6 – Design of the Water levitation pad

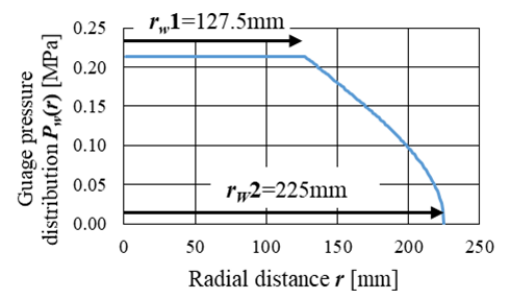


Fig. 7 – Gauge pressure distribution of water levitation pad



Next, the relationship between the levitation height h and the flow rate Q_w is shown in **Eq. (6)** where the viscosity of water is μ . The flow rate Q_w was determined by setting the levitation height h to the target value of 40 μm . Then, the flow rate Q_w became 1.5 L / min.

$$Q_w = \pi h_w^3 P_i / 6\mu_w \ln\left(\frac{r_w2}{r_w1}\right) \quad (6)$$

Assuming that the flow rate through the eight orifices is equal to Q_w , that is, the flow rate through the gap, the diameter d of the orifice was determined by the equation of nozzle as shown in **Eq. (7)**. The orifice coefficient α_w is set to 0.6 and ρ_w is the density of water. The supply pressure P_{ws} was set to a maximum pressure of 3 MPa of the plunger pump used in the experiment. The diameter d_w of the orifice was 0.4 mm.

$$Q_w/n = \alpha_w \left(\pi d^2 / 4 \right) \sqrt{2(P_{ws} - P_i) / \rho_w} \quad (7)$$

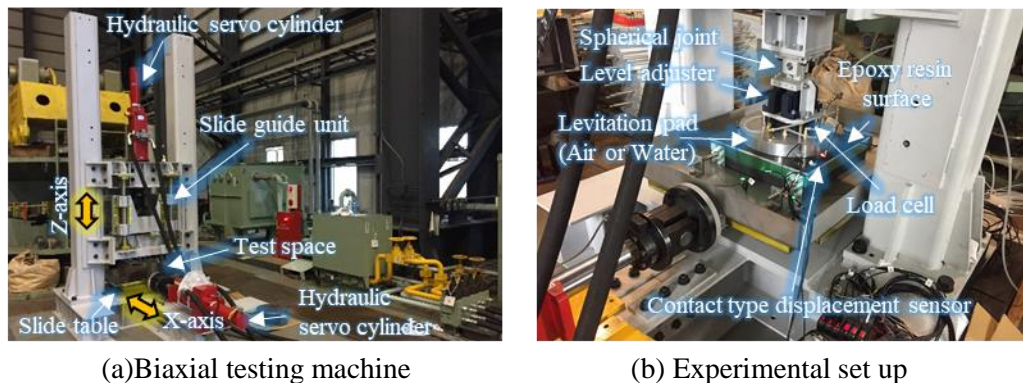
These design parameters are summarized in **Table 3**.

Table 3 – Parameter for design of water levitation pad

Item	Symbol	Value	Item	Symbol	Value
Support load	W	2,500 kg	Levitation pad diameter	$2 \cdot r_w2$	450 mm
Number of nozzles	n	8	Pocket diameter	$2 \cdot r_w1$	255 mm
Supply pressure (Gauge)	P_{ws}	3.0 MPa	Orifice diameter	d_w	0.4 mm
Orifice coefficient	α_w	0.6	Flow rate	Q_w	1.5 L/min
Water density	ρ_w	1,000 kg/m ³	Levitation height	h_w	40 μm
Water viscosity	μ_w	1.0×10^{-3} Pa sec			

4.3 Experiment outline

An experiment was conducted to confirm the function of the air levitation pad and the water levitation pad using the Biaxial Testing Machine. The Biaxial Testing Machine is a device uniquely designed by NIED consisting of two hydraulic cylinders with 5.19-kN (5-tonf) output vertically and horizontally perpendicular to each other, servo valve systems, a portal frame, and a slide guide unit. Static or dynamic load tests can be performed on the test specimen installed in the test space. The appearance of the experimental set up is shown in **Fig.8** and the specification of the biaxial testing machine and sensors are shown in **Table 4**. In this experiment, the pad was levitated at a constant fluid pressure, and the relationship between the supporting load, the fluid flow rate and the levitation height were monitored.



(a) Biaxial testing machine

(b) Experimental set up

Fig. 8 – Overview of the experiment for confirming the levitation height of the fluid levitation pad using a biaxial testing machine

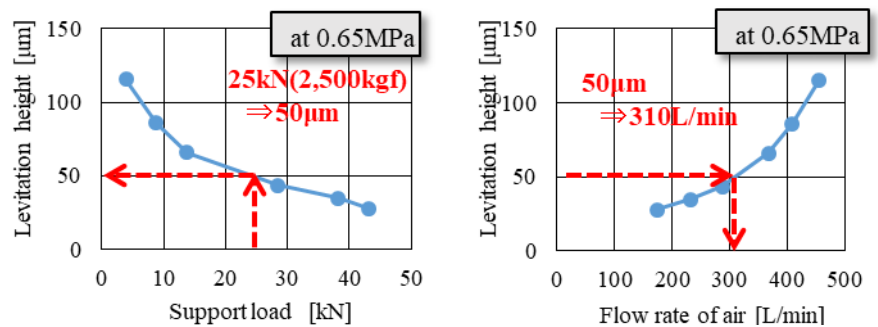


Table 4 – Specifications of biaxial testing machine and sensors

Item	Value	
Table size / Payload	70cm×70cm / 51.9kN (5 tonf) × 2-axis	
Shaking direction	X-horizontal	Z-vertical
Max. displacement	40 cm	10 cm
Load sensor	LTCE-A-100KN (F.S. 100kN), Kyowa Electronic Instruments	
Displacement sensor	GT2-S1(resolution ; 0.1μm, F.S. 1mm) , KEYENCE, (for levitation height)	
Pressure sensor	SEU11-6UA(F.S. 1MPa), PISCO & GC31(F.S. 5MPa), NAGANO KEIKI	
Gas flow sensor	PFMB7202-06-C-R(F.S. 2,000L/min), SMC	
Liquid flow sensor	PF3W704-03-AT-M-X143 (F.S. 4L/min), SMC	

4.4 Results in air levitation pad experiments

The experimental results of the air levitation pad are shown in Fig.9. The pressure was set to the design value of 0.65 MPa. At the support load of 25kN, the levitation height was about 50 μm, the flow rate was 310 L/min, which was almost the same as the design value so that the design method was verified.



(a) Support load and levitation height (b) Flow rate of air and levitation height

Fig. 9 – The experimental results of the air levitation pad

4.5 Results in water levitation pad experiments

The experimental results of the water levitation pad are shown in Fig.10. The flow rate was set to the design value of 1.5 L/min. At the supporting load of 25kN, the levitation height was about 28 μm. This levitation height was lower than expected, but if the orifice coefficient was adjusted experimentally, it would be possible to design a water levitation pad with this method. Although the target levitation height has not been satisfied, the excitation experiments were conducted with this setting due to the ability of the utility prepared this time.

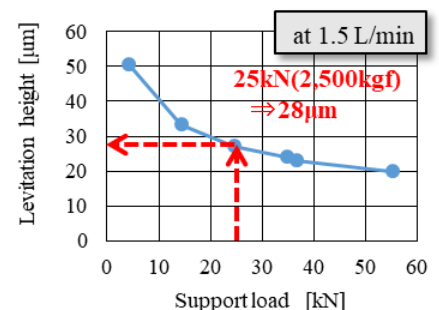


Fig. 10 – The experimental results of the water levitation

5. Experiment of seismic isolation system by E-Defense shaking table

5.1 E-Defense shaking table

E-Defense is the world's largest system capable of adding real seismic waves on a 1,200-ton-load specimen. By using E-Defense, excitation experiments of Prototype No.4 is performed. The test conditions are shown in Fig.11 and the specifications of E-Defense are shown in Table 5. It can reproduce the low-frequency components of the ground motion (up to a period of 10 seconds, and therefore the effects of seismic isolation can be verified.

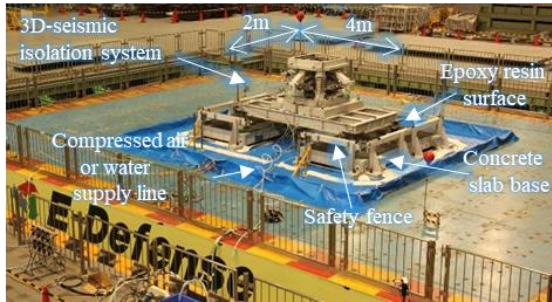


Fig. 11 – Installation of Prototype No.4 on E-Defense

Table 5 – Specification of E-Defense

Table size	15 × 20 m	
Payload	12 MN (1,200 tonf)	
Shaking direction	X,Y-horizontal	Z-vertical
Max. acceleration	900 cm/s ²	1500 cm/s ²
Max. velocity	200 cm/s	70 cm/s
Max. displacement	100 cm	90 cm

5.2 Configuration of Prototype No. 4

The equipment base was fixed on the shaking table. Compressed air and water for fluid levitation were supplied by tubes from compressors and pumps located outside of the shaking table. Accelerations are recorded at a sampling frequency of 1,000 Hz in the X, Y, and Z directions (NS, EW, and UD) with Accelerometers (JA5-V, Japan Aviation Electronics Industry) installed on the shaking table and the seismic isolation table. Three forms of Prototype No.4 are shown in **Table 6**. In this study, we performed excitation experiments on the cases of air and water as working fluids and changing the center of gravity. The seismic isolation system and the ground were moored by a soft coil spring so that the seismic isolation system could return to the center in order to perform the excitation experiments continuously. As a result, the target is not aperiodic, but the period is set to 10 seconds or more to prevent resonance with the main period component of the earthquake. On the other hand, in this case of no-center load, the seismic isolation system was expected to rotate due to the rectangular shape of the seismic isolation system and the experiment on the unbalanced load. The rotation of the seismic isolation system should be suppressed as much as possible to prevent wall collisions. Therefore, we tried to control the rotation by pulling the corner of the seismic isolation system at right angles with two wires.

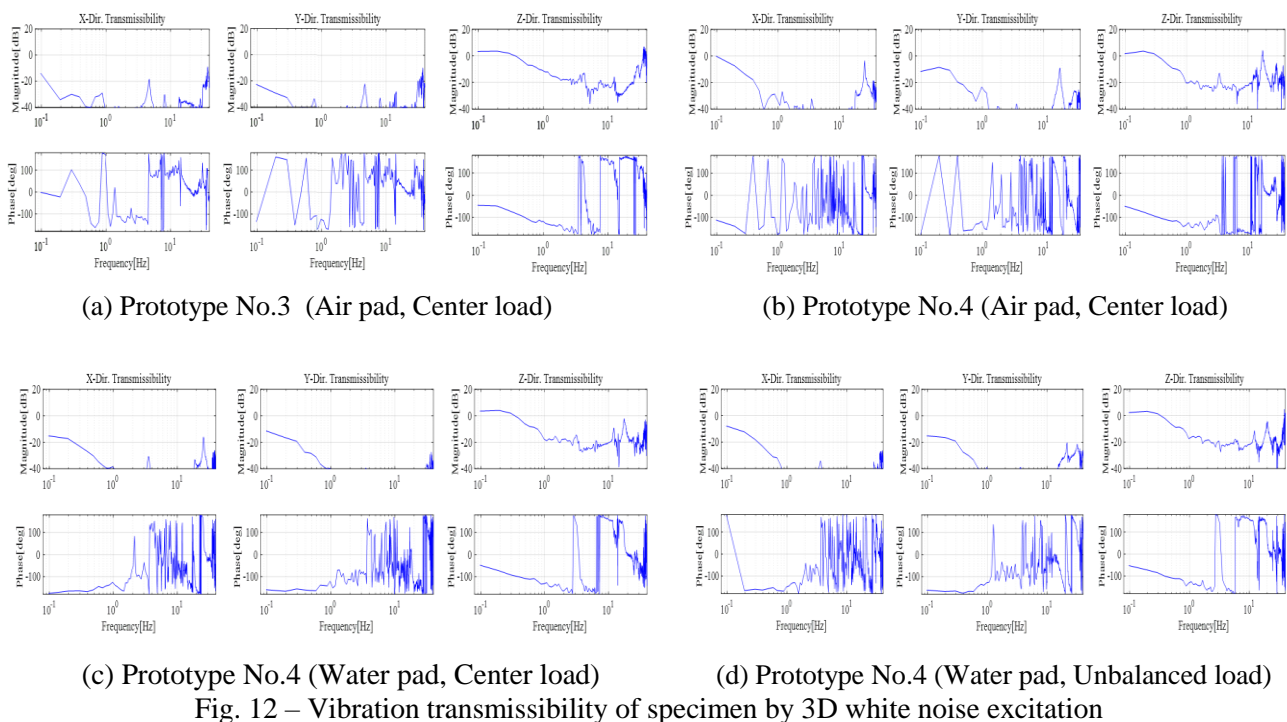
Table 6 – Three forms of Prototype No.4

Type	Air pad, Center load	Water pad, Center load	Water pad, Unbalanced load	
Overview				
Horizontal	Fluid	Air	Water	
	Load Position	Center	Center	
	Centering device			
	Period	10.2 sec	18.7sec	
	Dmping ratio	1.4%	4.5%	
Vertical	Prioad	4.5sec		
	Dmping ratio	12.0%		



5.3 White noise wave excitation

In order to understand the transfer characteristics of the seismic isolation device, we applied white noise waves with a maximum acceleration of 500 cm/s^2 and a frequency band of 0.5 to 35 Hz. The transfer characteristics obtained from the uni-axial excitation data between the shaking table and the seismic isolation system are shown in **Fig.12**. For comparison, (a) shows the results of the previous prototype No.3 and (b) to (d) show the results of Prototype No.4. In the horizontal direction, a good vibration reduction performance of -20 dB or less was obtained in the dominated frequency region of earthquakes (0.9 to 6.7 Hz[8]).



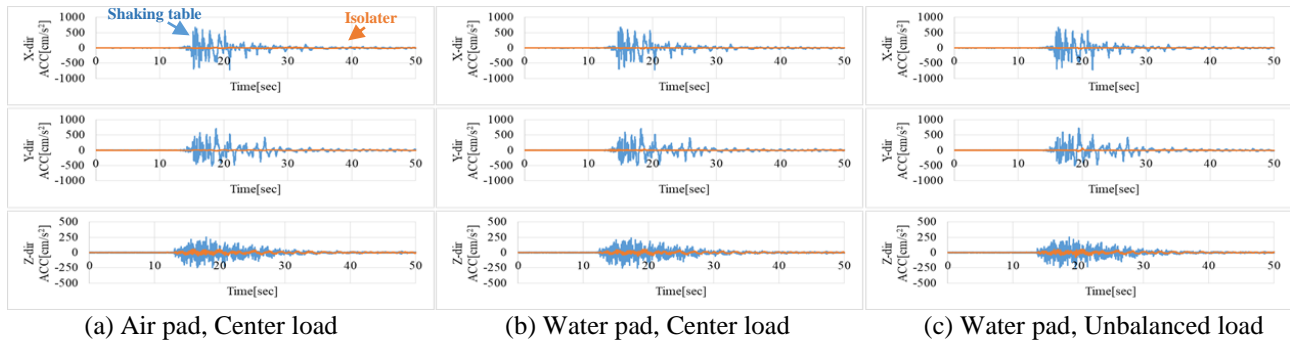
5.4 Actual and artificial seismic waves excitation

In order to confirm the performance of the seismic isolation system, excitation experiments were performed using actual seismic waves and artificial seismic waves. The actual seismic waves used were the 1995 Great Hanshin-Awaji Earthquake (JR Takatori [6]), the 2011 Tohoku-Pacific Ocean Earthquake (K-Net Sendai), and the 2016 Kumamoto Earthquake on April 16 (KiK-Net Mashiki-machi).

Two types of artificial seismic waves were created: inland earthquake type (Art. Inland) and trench earthquake type (Art. Trench). The two waves are generated in the following way: For the horizontal component of the artificial seismic wave, first, the target acceleration response spectrum considering the amplification by the surface ground was obtained from the acceleration response spectrum of the ground motion on the open engineering platform [7]. Acceleration time history waveforms were generated from the target acceleration response spectrum and the phase distribution of the actual seismic wave (inland earthquake: El Centro 1940 NS, trench earthquake: Hachinohe 1968 NS2). For the vertical component of the artificial seismic wave, the target acceleration response spectrum was the same as that of horizontal but multiplying the coefficient of vertical motion component [8]. Acceleration time history waveforms were generated from the target acceleration response spectrum and the phase distribution of the actual seismic wave (inland earthquake: El Centro 1940 UD, trench earthquake: Hachinohe 1968 UD2).

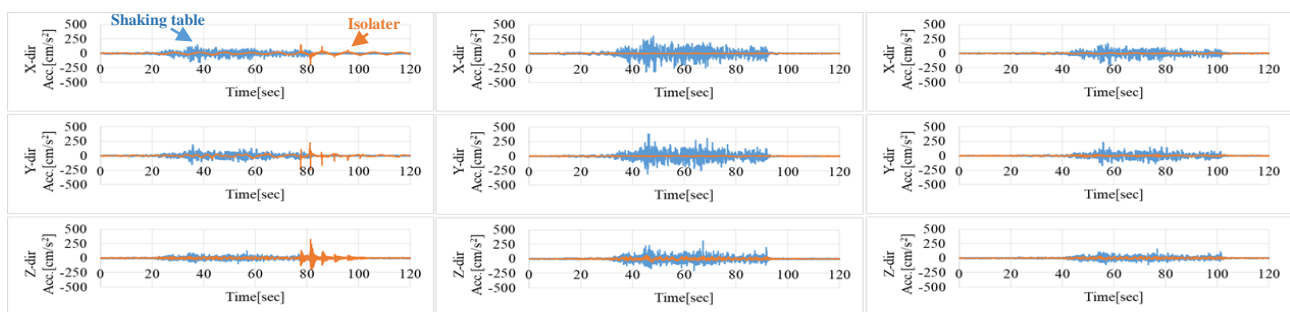


Experimental results under the excitation of JR Takatori is shown in **Fig.13**. Good results were obtained in which the maximum response acceleration in the horizontal direction was reduced to 1/10 or less and that in the vertical direction was reduced to 1/3 or less.



(a) Air pad, Center load (b) Water pad, Center load (c) Water pad, Unbalanced load
Fig. 13 – Time history by 3-D shaking of The 1995 Great Hanshin-Awaji Earthquake (JR Takatori) [6]

The acceleration time history of the trench-type artificial seismic wave is shown in **Fig.14**. In the air pad of (a), the horizontal centering mechanism became resonated because the natural frequency was around 10 seconds so that the isolation system collided with the retaining wall at the end of the excitation. In a water pad experiments, therefore, we changed the centering mechanism to a cross method. By this mean, the centering period was doubled and no collisions happened. The result of the water pad (b) was thus improved. The water pad (c) was input at 60% in consideration of the effect of offset load.



(a) Air pad, Center load (50% input) (b) Water pad, Center load (c) Water pad, Unbalanced load (60% input)
Fig. 14 – Time history by 3-D shaking of the artificial seismic waves of trench-type

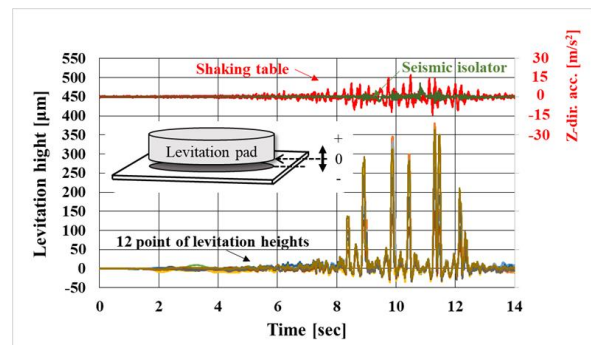
The maximum response acceleration, reduction rate, JMA measured seismic intensity, and JMA seismic intensity class in each direction on the shaking table and seismic isolation system are listed in **Table 7**. The blue letters indicate the cases that achieved the target seismic intensity class of 4 or smaller, and the red letters indicate the results of lower 5 of larger. It should be noted that the results of the Kumamoto earthquake show the seismic intensity of Upper 5 in all cases. Since the reduction rate is not different from other waveforms. This is because the input acceleration of the Kumamoto earthquake was too large, and the vertical acceleration even after vibration reduction exceeded $300 \text{ cm} / \text{s}^2$ (Gal). Therefore, it is necessary to improve the overall performance for further reduction. Note that the horizontal seismic isolation performance was generally good.



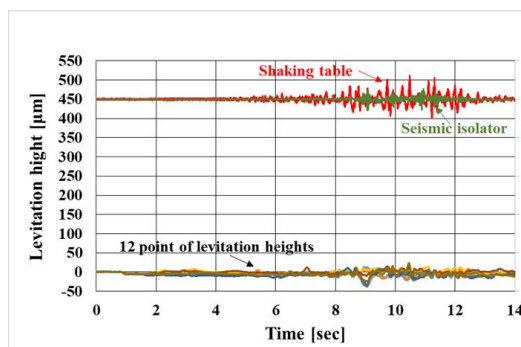
Table 7 – Maximum acceleration, reduction rate, measured seismic intensity and seismic intensity class

Model	Earthquake Wave	X-dir. Acc. [cm/s ²]			Y-dir. Acc. [cm/s ²]			Z-dir. Acc. [cm/s ²]			JMA measured seismic intensity		JMA seismic intensity class	
		Shaking Table	Iso-lator	Reduction rate[%]	Shaking Table	Iso-lator	Reduction rate[%]	Shaking Table	Iso-lator	Reduction rate[%]	Shaking Table	Iso-lator	Shaking Table	Iso-lator
Air pad, Center load	JR Takatori	723	19	97.4	708	22	96.9	255	59	77.1	6.4	3.8	Upper6	4
	Sendai 50%	436	11	97.5	797	14	98.2	165	36	78.4	5.7	3.4	Lower6	3
	Kumamoto	1,569	142	91.0	1,055	85	91.9	1,519	543	64.2	6.5	5.2	7	Upper5
	Art. Inland 50%	259	121	53.2	213	323	-51.8	202	318	-57.5	5.0	5.6	Upper5	Lower6
	Art. Trench 50%	156	202	-29.7	194	239	-23.1	123	321	-161.1	4.9	5.3	Lower5	Upper5
Water pad, Center load	JR Takatori	717	34	95.3	723	66	90.9	257	79	69.5	6.4	4.3	Upper6	4
	Sendai	914	10	98.9	1,740	6	99.6	375	47	87.3	6.3	3.7	Upper6	4
	Kumamoto	1,654	159	90.4	1,007	115	88.5	1,479	386	73.9	6.5	5.1	7	Upper5
	Art. Inland	541	29	94.6	439	9	98.0	443	85	80.9	5.6	3.8	Lower6	4
	Art. Trench	318	7	97.8	381	9	97.6	310	63	79.5	5.5	3.9	Lower6	4
Water pad, Edge load	JR Takatori	712	33	95.3	716	38	94.7	252	61	75.9	6.4	3.9	Upper6	4
	Sendai	911	8	99.1	1,741	41	97.6	376	53	85.8	6.3	3.6	Upper6	4
	Kumamoto	1,584	79	95.0	1,082	84	92.3	1,518	363	76.1	6.6	5.0	7	Upper5
	Art. Inland 60%	315	11	96.4	254	21	91.9	232	45	80.4	5.5	3.4	Upper5	3
	Art. Trench 60%	189	12	93.4	229	24	89.5	159	31	80.5	5.0	3.5	Upper5	4

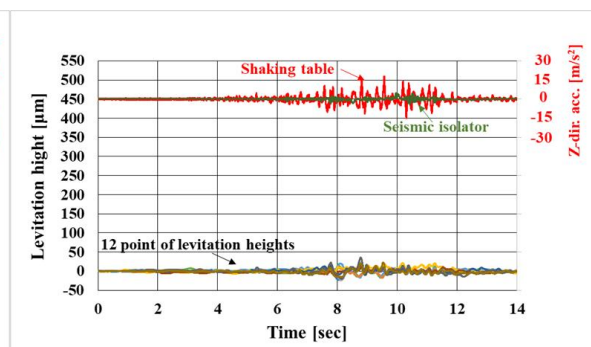
The time history of the levitation height of the fluid levitation pad during the Kumamoto earthquake is shown in Fig.15 in which the highest vertical acceleration in this experiment was inputted. The upper part of the figure shows the vertical shaking table acceleration and the response acceleration of the seismic isolation system. The levitation heights in this figure are under assumption that the levitation positions before excitation are zero. No impact was generated at the timing of the input acceleration of 15m / s² (1,500 Gal) or more and therefore it is considered that the fluid levitation pad did not contact the floor. It should be noted that the air pad detected a bounce close to 400 μm (0.4 mm). This record is very large by comparing with the last Prototype No.3 experiment results of heights within 50μm in the same case [5]. However, in Prototype 3, the glass plate used for the base might be deformed, and the apparent levitation height was possibly reduced by following the pad, so that it may not have been exposed. The cause of large bounces in Prototype No.4 is considered to be that the movable range in the pad was widened by using the spherical seat and the pad was allowed to vibrate due to the compressibility of air. However, since the pad is provided with an orifice to increase the vertical rigidity, a theoretical confirmation will be made in the future. Note that a clear performance difference was not observed from the response acceleration. In comparison, the incompressible water system was found to be operating very stably.



(a) Air pad, Center load



(b) Water pad, Center load



(c) Water pad, Unbalanced load

Fig. 15 – Time history by 3-D shaking of The 2016 Great Kumamoto earthquake (KiK-net Mashiki-machi)



6. Conclusions

We have developed a 3D seismic isolation system characterized by connecting a coil spring and a negative rigid link in parallel on a fluid levitation pad using air or water. A seismic excitation experiment was performed by the 3D Full-Scale Earthquake Testing Facility (E-Defense). The support load of the horizontal seismic isolation system is 10 tons, and the support load is 2 tons in vertical. As a result, it was confirmed that the horizontal acceleration can be reduced to less than 1/10 of the input and the vertical acceleration can be reduced to less than 1/3 of the input for almost of all excitation waves. In addition, the seismic intensity 4 or less was achieved on the seismic isolation system for the input of JR Takatori [6], K-net Sendai, and two types of artificial seismic waves, inland type and trench type. The period of the horizontal centering mechanism affected the experimental results, and the main body collided with the retaining wall due to some excitation waves. However, by increasing the centering period, the retaining wall collision was avoided, and the vibration reduction performance was improved.

A comparison was made between air and water as the levitation fluid. As a result of the excitation experiment, there was no clear difference in performance, and there was no contact between the pad and the floor surface at an input acceleration exceeding 15 m/s^2 (1,500 Gal). When a large vertical acceleration was applied, the air pads bounced to about $400 \mu\text{m}$, but it did not affect the vibration elimination performance. On the other hand, the height variation of the water pad was stable at about $\pm 30 \mu\text{m}$. In the future, we will consider increasing the capacity based on these results. As a next step, we plan to develop larger size of systems for actual applications.

7. References

- [1] Cabinet Office Japan: White Paper on Disaster Management 2019
- [2] Masashi YASUDA, Eiji SATO, Manabu YAMADA, Koichi KAJIWARA, Masaki HAYATSU (2017): Development of three-dimensional seismic isolation system using negative stiffness link mechanism and air levitation mechanism in series. *Transactions of the JSME* (in Japanese), Volume 83 Issue 851 Pages 17-00057.
- [3] Masashi YASUDA, Eiji SATO, Manabu YAMADA, Koichi KAJIWARA, Masaki HAYATSU (2017): Development of three-dimensional seismic isolation system realizing horizontal periodicity by air levitation. *Transactions of the JSME* (in Japanese), Volume 84 Issue 861 Pages 17-00509
- [4] Manabu YAMADA, Koichi KAJIWARA, Eiji SATO, Masaki HAYATSU, Hideo KASE, Masashi YASUDA (2018): Development of three-dimensional seismic isolation system using air levitation, negative stiffness link and air dumper. *Dynamics and Design Conference 2018*, 226. jsmedmc.2018.226 (in Japanese)
- [5] Manabu YAMADA, Koichi KAJIWARA, Eiji SATO, Masaki HAYATSU, Hideo KASE, Masashi YASUDA (2019): Experimental validation about the behavior of the elements in three-dimensional seismic isolation system by air levitation. *Dynamics and Design Conference 2019*, 234. jsmedmc.2019.234 (in Japanese)
- [6] Nakamura, Y., Uehan, F. and Inoue, H. : Waveform and its Analysis of the 1995 Hyogo-Ken-Nanbu Earthquake (II), JR Earthquake Information No. 23d, *Railway Technical Research Institute*, March 1996 (in Japanese)
- [7] Ministry of Construction Notification No. 1461 (2000) (in Japanese)
- [8] Technical guideline for creating input seismic ground motion for design (draft), The Building Center of Japan (1992) (in Japanese)